ASEAN Engineering Journal

Full Paper

REDUCTION OF AMMONIACAL NITROGEN AND CHEMICAL OXYGEN DEMAND VIA PILOT-SCALE PHOTOCATALYTIC REACTOR INCORPORATED WITH ZNO-KAOLIN

Mohamad Alif Hakimi Hamdan[a], Rais Hanizam Madon[b*], Nur Hanis Hayati Hairom[a,c], Siti Nurfatin Nadhirah Mohd Makhtar[c], Mohd Khairul Ahmad[c], MZahar Abd Jalal[b]

[a]Faculty of Engineering Technology, Universiti Tun Hussein Onn Malaysia, Hab Pendidikan Tinggi Pagoh, KM1, Jalan Panchor, 84600 Muar, Johor, Malaysia
[b]Faculty of Mechanical and Manufacturing Engineering, Universiti Tun Hussein Onn Malaysia, 86400, Parit Raja, Batu Pahat, Johor, Malaysia
[c]Microelectronics and Nanotechnology–Shamsuddin Research Centre (MiNT-SRC), Institute for Integrated Engineering, Universiti Tun Hussein Onn Malaysia, 86400, Parit Raja, Batu Pahat, Johor, Malaysia

Article history
Received
21 May 2024
Received in revised form
08 August 2024
Accepted
13 August 2024
Published online
31 August 2025

*Corresponding author
raismadon@uthm.edu.my

Graphical abstract

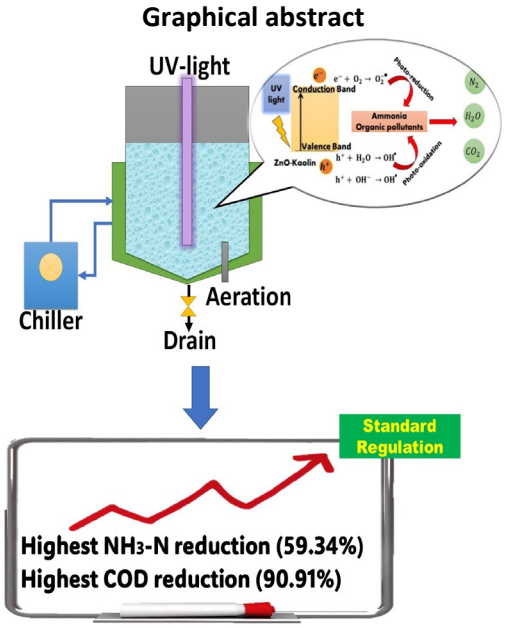

Abstract

Photocatalytic is an advanced technology for water remediation which potentially to be applied for river pollution treatment. The key to the highest photocatalytic efficiency is the type of photocatalyst used and the process variables including light sources, light intensity, and time operations. However, the study on the interaction of process variables on photocatalytic efficiency for polluted river water treatment has not been well studied. Thus, the present study focused on the performance of pilot-scale photocatalytic reactor incorporated with ZnO-Kaolin under various light intensities such as 100, 125, and 225 Watts with varied time operation at 20, 40, 60 and 80 minutes for reduction of ammoniacal nitrogen (AN) and chemical oxygen demand (COD). Followed by the elucidation of kinetic study through pseudo-first and pseudo-second-order models. It was found that 225 Watts of UV-light contributed to the highest reduction of AN (59.34%) and COD (90.91%) for 60 minutes of treatment. Furthermore, the kinetic study revealed that the photocatalytic process follows pseudo-first-order model with a rate constant of 0.0184 min^{-1}. Hence, the highest photocatalytic efficiency of ZnO-Kaolin is mainly attributed to the intensive light intensity, leading to the higher generation of reactive species for rapid photocatalytic degradation, consequently improving the performance of pilot-scale photocatalytic reactor.

Keywords: River water, Polluted, Photocatalysis, Pilot-scale, Environment
.

1.0 INTRODUCTION

Urbanization and modernization lead to river water pollution, which creates severe problems for the sustainability of water resources. The river in Malaysia facing major challenges especially in terms of Biochemical Oxygen Demand (BOD), Ammoniacal Nitrogen (NH_3-N), and Suspended Solids (SS) [1]. Many efforts have been devoted to the remediation of polluted river water, including physical, chemical, biological, ecological, and engineering techniques [2]. Recently, photocatalytic degradation has emerged as a superior treatment technology, especially when compared to electrocoagulation, membrane bioreactor (MBR), and conventional biological processes such as activated sludge. From both technical and environmental perspectives, photocatalysis offers high efficiency in removing a wide range of pollutants, including organic and inorganic matter. This method consistently outperforms conventional

biological processes under optimal conditions, while electrocoagulation and MBR systems require more complex operations and frequent maintenance. Moreover, photocatalysis is environmentally friendly and capable of degrading a wide range of pollutants with minimal environmental impact. Economically, photocatalytic processes are more cost-effective in the long term due to their rapid treatment capabilities, significantly reducing operational time and associated costs. In contrast, electrocoagulation and MBR systems incur substantial operating expenses related to energy consumption and maintenance, making them less economically viable over time [3]–[6].

It was reported that the performance of photocatalytic degradation is highly influenced by process variables, such as type of photocatalyst, light intensity and time operation [7]. Previously 90% degradation of organic and inorganic compounds was achieved using ZnO photocatalysts, owing to the highly photosensitive and oxidative properties of ZnO [8], [9]. Nonetheless, ZnO properties can be further improved by embedding with kaolin, as pure ZnO tends to agglomerate. The combination of ZnO and kaolin has been reported to improve the active site and effectively prevent the agglomeration of ZnO nanoparticles [10]. Moreover, kaolin is widely used as a supporting material for ZnO nanoparticles due to its adsorption behaviour, chemically and mechanically stable [11], [12].

To the best of the authors' knowledge, a pilot-scale study for polluted river water remediation via photocatalytic degradation process has not been establish yet which brings to the fact that studying the stability and process variables of pilot-scale photocatalytic systems is crucial to investigate the behaviour of the process on a large scale. Hence, this study provides an investigation on photocatalytic degradation for river water remediation which focuses on the optimization of light intensity and operation time. The outcome would give a best picture in relating the process variables with the photocatalytic degradation performance.

2.0 MATERIALS AND METHODS

This section discussed the procedure for sampling the polluted river water, synthesis the ZnO-Kaolin photocatalyst, and characterize its properties. Followed by set-up operation for the pilot-scale photocatalytic reactor, analysis of the treated water and the kinetic study.

2.1 Polluted River Water Sampling

The polluted river water samples were directly collected from Sungai Sembrong, Parit Raja and characterized through ammoniacal nitrogen (AN) and chemical oxygen demand (COD) by using DR6000 UV-Vis Spectrophotometer according to the standard method of 8038 and 8000, respectively. From the investigation, the river water has an AN of 2.41 mg/L and COD of 55 mg/L. It proved that this targeted river highly contained ammonia and organic pollutants for which further treatment is required.

2.2 Synthesis Of Zno-Kaolin

ZnO-Kaolin was synthesised through the precipitation method using zinc acetate dihydrate, oxalic acid dihydrate, and kaolin powder purchased from R&M Marketing Essex, UK and used as it. A solution of 0.1M of zinc acetate and 0.15M of oxalic acid was mixed with 33.33 g/L of kaolin powder. Then, the mixture was stirred for 24 hours, filtered, dried, and calcined at 550°C for 3 hours. The resulting white powder was collected for further analysis.

2.3 Characterization Of Zno-Kaolin

The functional group and crystallinity of the ZnO-Kaolin were individually analyzed through Perkin Elmer Spectrum 100 Fourier Transform Infrared Spectroscopy (FTIR) Spectrum and Bruker AXS GmbH X-ray diffractometer (XRD), respectively. The optical band gap of the ZnO-Kaolin was performed by UV-Vis Diffuse Reflectance Spectra (UV 3600 Plus).

2.4 Pilot-Scale Photocatalytic Reactor And Experimental Set-Up

The pilot-scale photocatalytic reactor has a volume capacity of 80L and is equipped with an ultraviolet-C (UV-C) lamp (wavelength: 280 nm). A blower was installed in the reactor for mixing and aeration. The photocatalytic reactor is also equipped with a cooling jacket connected to a chiller to maintain a mild temperature during the treatment. At first, 80 L of the samples were fed to the photocatalytic reactor with 5% wt of ZnO-Kaolin photocatalyst. The blower was engaged to mix the solution and photocatalyst for effective adsorption-desorption. After that, the UV light was activated to run the photocatalytic process. The treated sample was collected for further analysis. Various UV light power (100, 125 and 225 Watts) and time operations (20 - 80 minutes) were conducted to optimize the process condition. Figure 1 shows the set-up of the pilot-scale photocatalytic reactor.

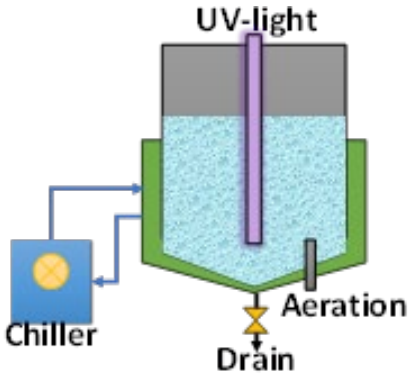

Figure 1 Pilot-scale photocatalytic reactor set-up experiment

2.5 Analysis Of The Water Quality

The efficiency of the treatment was evaluated through the percentage removal of AN and COD after the treatment by using the Eq. 1:

$$\text{Efficiency} = (C_0 - C_t)/C_0 \times 100\% \quad (1)$$

where, C_o is the water quality before the treatment, C_t is the water quality after the treatment.

2.6 Kinetic Study

Pseudo-first and pseudo-second-order models were suggested to investigate the kinetic study for the pilot-scale photocatalytic reactor. The integrated forms of the pseudo-first and pseudo-second-order models are according to Eq. 2 and Eq. 3, respectively.

$$\ln (C_o/C_t) = kt \quad (2)$$

$$1/C_t = 1/C_o + kt \quad (3)$$

where C_o is the initial concentration of the pollutant, C_t is the concentration of the pollutants at time, and k is the rate constant.

3.0 RESULTS AND DISCUSSION

This section will further discuss the findings of this study. There are 3 components that have been discovered which are ZnO-Kaolin characterization, optimization of pilot-scale photocatalytic reactor and kinetic study.

3.1 Characterization Of Zno-Kaolin

Figure 2a shows the XRD pattern for ZnO-Kaolin. It was observed that the peaks of ZnO were detected well as the standard ZnO according to JCPDS no. 36-1451. The detected peaks were <100>, <002>, <102>, <110> and <103> at 31.8°, 36.3°, 33.1°, 56.6°, 63.1° and 68.1°, respectively. These peaks correspond to crystallographic orientations of the ZnO wurtzite structure [13]. While the presence of kaolinite structure was found at <001>, <002>, <020> and <021> at 12°, 24.5°, 35.5°, and 39.5° according to JCPDS no. 14-0165. It could be concluded that the synthesized ZnO-Kaolin has higher purity. Besides, the FTIR spectra of ZnO-Kaolin have been illustrated in Figure 2b. The FTIR analysis was conducted within the wavenumber of 400 – 4000cm^{-1}. From the observations, the region of metal oxide, Zn-O stretching vibration probably occurs in the range of 500 – 1000 cm^{-1} [14], [8]. Additionally, within this range also exhibits kaolinite compounds which are silicate and aluminates (Si-O-Al). Moreover, bands around 1040-1080 cm^{-1} correspond to silicate (Si-O) stretching vibrations. The broad bands within 3000 – 37000 cm^{-1} are associated to hydroxyl (O-H) stretching vibrations due to moisture in the atmosphere [15]. This finding proved that the synthesized ZnO-Kaolin contains only a selective compound. On the other hand, the graph in Figure 2c represents Tauc plots for determining the optical band gap of the ZnO-Kaolin. The extrapolation of the tangent line in the graph corresponds to the value of the optical band gap, which is 3.23 eV. It was reported that the optical band gap of ZnO is typically within the range of 3.10 eV to 3.37 eV [16]. The obtained optical band gap is slightly low and within the range, which means that ZnO-Kaolin has great potential in photocatalytic degradation. Figure 3 illustrates the distribution of ZnO nanoparticles on the kaolin matrix using FESEM. The FESEM image reveals a layered, flat-sheet shape with the attachment of an oval shape corresponding to kaolin and ZnO nanoparticles, respectively. Similarly, Awang et al. also observed a flake-like shape for ZnO-Kaolin using FESEM [17]. Overall, the FESEM findings highlight that no agglomeration of ZnO nanoparticles was found and distributed evenly.

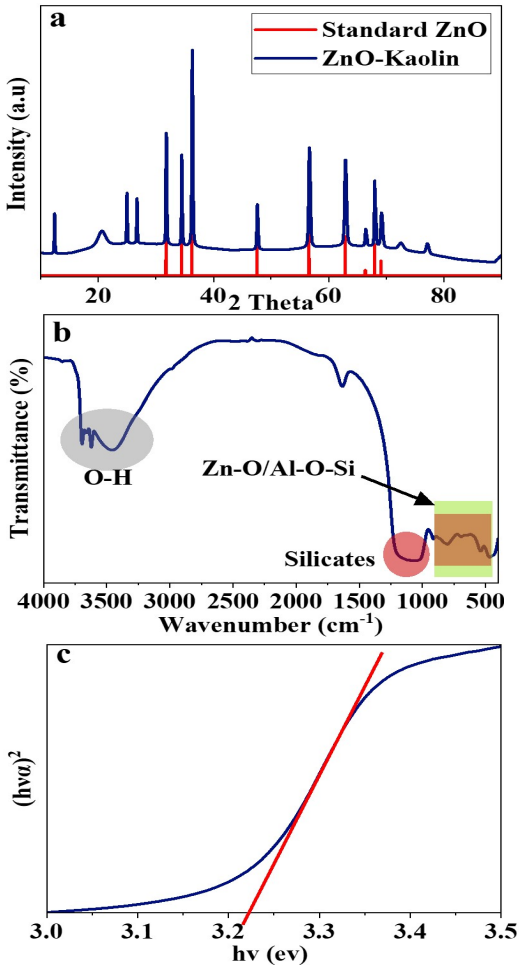

Figure 2 Analysis of ZnO-Kaolin through: (a) XRD, (b) FTIR, and (c) optical band gap

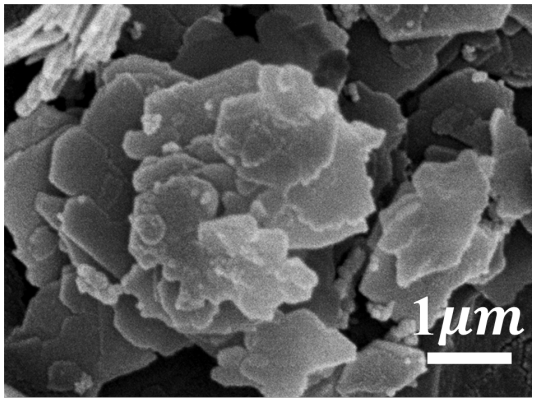

Figure 3 FESEM image of ZnO-Kaolin

3.2 Optimization Of Pilot-Scale Photocatalytic Reactor

The optimization of the pilot-scale photocatalytic reactor was studied across various UV-light power and time operations as illustrated in Figure 5. Figure 5(a) revealed the interaction of various UV-light powers (100, 125 and 225 Watts) to photocatalytic efficiency. It was observed that the elevation of UV-light power exhibited an increase in pollutant reduction. The power of 225 Watts UV-light corresponded to the highest reduction of AN and COD by 59% and 90%, respectively. This phenomenon is due to the utilization of UV-C with intensive power. Intensively applied power contributes to higher light intensity, which triggers excessive photons for electron mobility within the ZnO-Kaolin, consequently heightening the amount of reactive radical species, such as hydroxyl radical and superoxide radical for greater oxidation of ammonia and organic compounds [18]. The mechanism for photocatalytic degradation of pollutants has been illustrated in Figure 4. Additionally, the presence of ZnO-Kaolin enhanced photocatalytic degradation by having a lower optical band gap (3.23 eV) to suppress electron recombination. Moreover, merging ZnO with Kaolin improved the adsorption rate of pollutants to reach the ZnO active site for rapid oxidation [19].

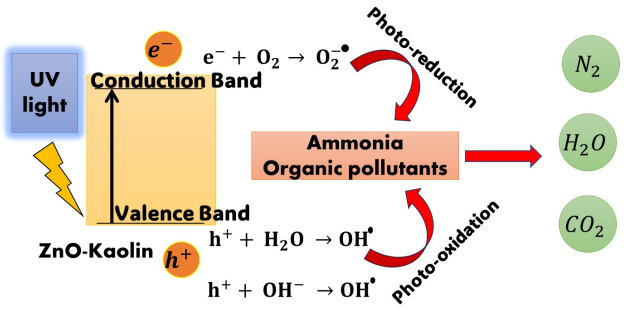

Figure 4 Photo-degradation mechanism of ZnO-Kaolin

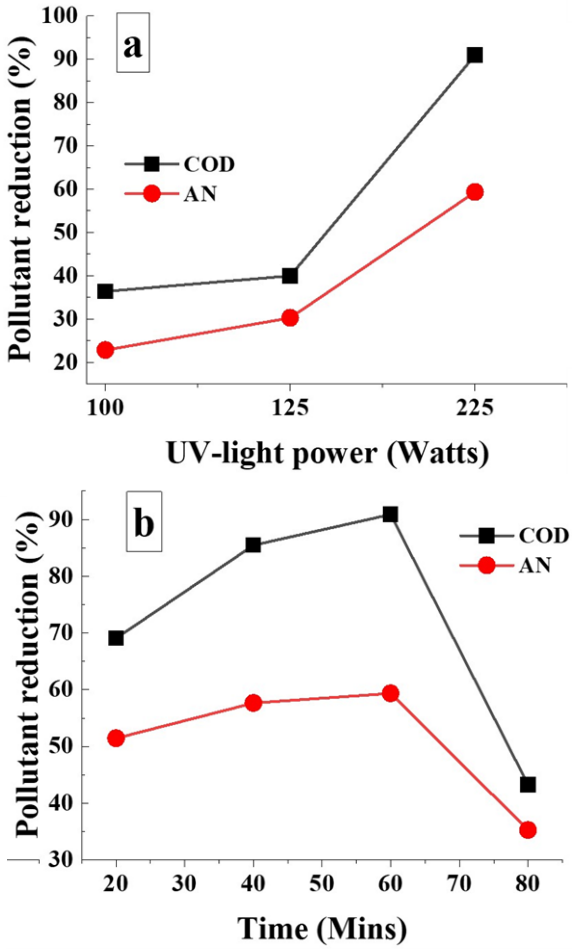

Figure 5 Performance of pilot-scale photocatalytic reactor under various conditions: (a) UV-light power and (b) time operations

Besides, the interaction of time operation on the performance of pilot-scale photocatalytic reactor for the reduction of pollutants is illustrated in Figure 4(b). The graph shows that 60 minutes yields the highest reduction of AN and COD by 59.34% and 90.91%, respectively. A gradual increase in ammonia nitrogen (AN) and chemical oxygen demand (COD) reduction was observed from 20 min to 60 min. This phenomenon was influenced by the increased amount of reactive oxidative species, leading to higher photocatalytic degradation. However, beyond 60 min, the efficiency of the photocatalytic process decreases significantly. This is probably due to the photocatalyst reaching its maximum photon absorption capacity, especially within the ZnO-Kaolin. At this point, the generation of reactive oxidative species becomes insufficient to maintain the high rate of pollutant degradation. This saturation effect occurs when all available active sites on the photocatalyst are occupied, causing the rate of electron-hole pair formation to stabilize and leading to a reduction in the overall photocatalytic activity [13]. The photocatalytic efficiency of different ZnO was briefly summarized in Table 1.

Table 1 Summary of photocatalytic efficiency of different ZnO photocatalysts.

Water matrices	Photocatalyst	Light source	Efficiency	Remarks	Ref
Aquaculture wastewater	Nano-ZnO	UV irradiation	AN reduction: 86.66% (1h); COD reduction: n	*in presence of H_2O_2 to achieve high efficiency	[20]
Domestic wastewater	Cu/ZnO/rGO	Xenon light Irradiation (120 watt)	AN reduction: 83.1% (2h); COD reduction: 84.3% (2h)	*Required complex catalyst synthesis method	[21]
Aerobically palm oil mill effluent	ZnO-CC (Cymbopogon Citratus)	UV-light irradiation	AN reduction: n; COD reduction: 75.4% (60 min)	*Required plant extraction to synthesis catalyst *Conducted at small-scale (2 L)	[22]
Sago wastewater effluent	ZnO	UV-light irradiation (8 watt)	AN reduction: n; COD reduction: 90% (2h)	*Conducted at small-scale (150 mL) *Required pre-treatment 2 h of aeration to achieve high reduction of COD	[23]
Polluted river water	ZnO-Kaolin	UV-light (225 watt)	AN reduction: 59% (60min); COD reduction: 90% (60min)	*Simple preparation of catalyst *Conducted at pilot-scale (80 L)	This work

*n indicates no info was provided

3.2 Kinetic Study

The kinetic study on photocatalytic degradation via pilot-scale photocatalytic reactor was studied for its optimum conditions based on pseudo-first and pseudo-second-order models. Figure 6 displays the graph of pseudo-first and pseudo-second-order models. It was found that pseudo-first-order model was applicable due to the highest value of R^2 (0.9118) with a rate constant of 0.0184 min^{-1}. The pseudo-first-order model defined that the photocatalytic degradation rate is proportional to the concentration of the pollutants, typically the limiting reactant [24].

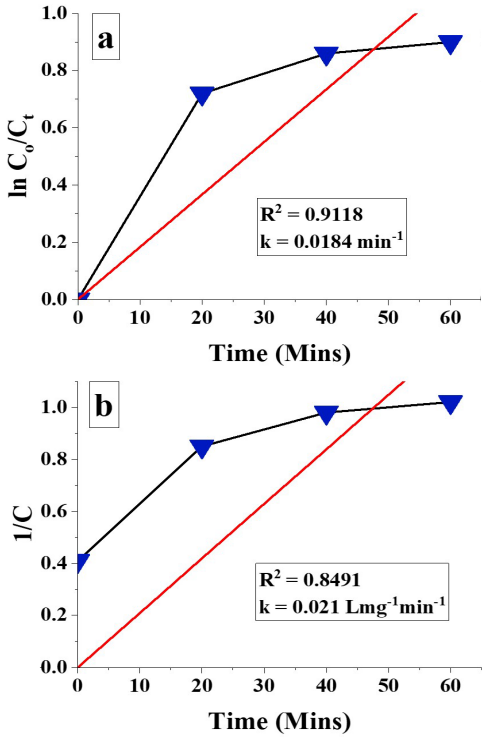

Figure 6 Graph of (a) Pseudo-first-order model and (b) Pseudo-second-order model

4.0 CONCLUSION

This study revealed an advanced photocatalytic system for polluted river water treatment. The performance of a pilot-scale photocatalytic reactor incorporated with ZnO-Kaolin for polluted river water remediation has been successfully evaluated under different operating conditions such as light intensity and time operation. From the findings, 225 Watts of UV-light yielded the highest reduction of AN and COD by 59.34% and 90.91%, respectively for 60 minutes of treatment. Moreover, a kinetic study revealed that pseudo-first-order models are applicable for this treatment due to the highest correlation coefficient (R^2) value obtained with a rate constant (k) of 0.0184 min^{-1}. It revealed the photocatalytic degradation rate is proportional to the concentration of pollutants. Therefore, a pilot-scale photocatalytic reactor is believed to have great potential in maintaining environmental sustainability and approaching sustainable development goals (SDG 6) in sustaining water and sanitation availability and sustainable management.

Acknowledgement

This research was supported by the Ministry of Higher Education (MOHE) through Fundamental Research Grant Scheme (FRGS/1/2021/WAB05/UTHM/02/1). The authors also gratefully acknowledge the technical and administrative support from Universiti Tun Hussein Onn Malaysia (UTHM).

Conflicts of Interest

The author(s) declare(s) that there is no conflict of interest regarding the publication of this paper

References

[1] C. Lee Goi, 2020. "The river water quality before and during the Movement Control Order (MCO) in Malaysia," *Case Studies in Chemical and Environmental Engineering*, 2: 100027, DOI: 10.1016/j.cscee.2020.100027.

[2] N. H. H. Hairom et al., 2021. "A review of nanotechnological applications to detect and control surface water pollution," *Environmental Technology and Innovation,* 24: 102032, DOI: 10.1016/j.eti.2021.102032.

[3] M. Pavel, C. Anastasescu, R. N. State, A. Vasile, F. Papa, and I. Balint, 2023. "Photocatalytic Degradation of Organic and Inorganic Pollutants to Harmless End Products: Assessment of Practical Application Potential for Water and Air Cleaning," *Catalysts,* 13(2): 380, DOI: 10.3390/catal13020380.

[4] N. S. A. Mutamim, Z. Z. Noor, M. A. A. Hassan, A. Yuniarto, and G. Olsson, 2013. "Membrane bioreactor: Applications and limitations in treating high strength industrial wastewater," *Chemical Engineering Journal,* 225: 109–119. DOI: 10.1016/j.cej.2013.02.131.

[5] B. Rezai and E. Allahkarami, 2021, "Wastewater Treatment Processes—Techniques, Technologies, Challenges Faced, and Alternative Solutions," in *Soft Computing Techniques in Solid Waste and Wastewater Management,* 1: 53–77. DOI: 10.1016/B978-0-12-824463-0.00004-5.

[6] S. Akter, M. B. K. Suhan, and M. S. Islam, 2022. "Recent advances and perspective of electrocoagulation in the treatment of wastewater: A review," *Environmental Nanotechnology, Monitoring and Management*, 17: 100643, DOI: 10.1016/j.enmm.2022.100643.

[7] S. Ahmed, M. G. Rasul, R. Brown, and M. A. Hashib, 2011. "Influence of parameters on the heterogeneous photocatalytic degradation of pesticides and phenolic contaminants in wastewater: A short review," Journal of Environmental Management, 92(3): 311–330, DOI: 10.1016/j.jenvman.2010.08.028.

[8] M. A. H. Hamdan et al., 2020. "Catalytic conversion of synthetic sulfur-pollutants in petroleum fractions under different photocatalyst loadings and initial concentration," International Journal of Emerging Trends in Engineering Research, 8(1.2): 132–138, DOI: 10.30534/ijeter/2020/1881.22020.

[9] D. A. B. Sidik, N. H. H. Hairom, M. K. Ahmad, R. H. Madon, and A. W. Mohammad, 2020. "Performance of membrane photocatalytic reactor incorporated with ZnO-Cymbopogon citratus in treating palm oil mill secondary effluent," *Process Safety and Environmental Protection,* 143: 273–284, DOI: 10.1016/j.psep.2020.06.038.

[10] A. Mohagheghian, S. H. Rad, K. Ayagh, and M. Shirzad-Siboni, 2022. "Photocatalytic Removal of Acid Blue 113 Dye from Aqueous Solutions Using Zinc Oxide-Kaolin Nanocomposite under Visible Light Irradiation," *Journal of Mazandaran University of Medical Sciences,* 32(209): 60–70,

[11] M. Chen et al., 2023. "The Application of Mineral Kaolinite for Environment Decontamination: A Review," *Catalysts*, 13(1): 123, DOI: 10.3390/catal13010123.

[12] S. Ahmad and N. Shoukat, 2024. "Synthesis of cerium doped ZnO/kaolin photocatalysts for the purification of pharmaceutical wastewater," *Journal of Materials Science,* 59(1): 154–168, DOI: 10.1007/s10853-023-09145-4.

[13] S. H. Ummi Kalsum Hasanah Mohd Nadzim, Nur Hanis Hayati Hairom, Mohamad Alif Hakimi Hamdan, Mohd Khairul Ahmad, Aishah Abdul Jalil, Nurfatehah Wahyuny Che Jusoh, 2022. "Effects of different zinc oxide morphologies on photocatalytic desulfurization of thiophene," *Journal of Alloys and Compounds,* 913: 165145, DOI: 10.1016/j.jallcom.2022.165145.

[14] A. H. Zyoud et al., 2019. "Kaolin-supported ZnO nanoparticle catalysts in self-sensitized tetracycline photodegradation: Zero-point charge and pH effects," *Applied Clay Science,* 182: 105294, DOI: 10.1016/j.clay.2019.105294.

[15] S. Modi et al., 2023. "Photocatalytic Degradation of Methylene Blue from Aqueous Solutions by Using Nano-ZnO/Kaolin-Clay-Based Nanocomposite," *Water,* 15(22): 3915, DOI: 10.3390/w15223915.

[16] K. Davis, R. Yarbrough, M. Froeschle, J. White, and H. Rathnayake, 2019. "Band gap engineered zinc oxide nanostructures: Via a sol-gel synthesis of solvent driven shape-controlled crystal growth," *RSC Advances*, 9(26): 14944–14953, DOI: 10.1039/c9ra02091h.

[17] Z. Awang et al., 2024. "Palm oil mill secondary effluent treatment using ZnO-clay liquid photocatalyst in membrane photocatalytic reactor," *Journal of the Indian Chemical Society*, 101(7): 101158, DOI: 10.1016/j.jics.2024.101158.

[18] M. Yousefi, M. Farzadkia, A. H. Mahvi, M. Kermani, M. Gholami, and A. Esrafili, 2024. "Photocatalytic degradation of ciprofloxacin using a novel carbohydrate-based nanocomposite from aqueous solutions," *Chemosphere,* 349: 140972, DOI: 10.1016/j.chemosphere.2023.140972.

[19] T. Gul et al., 2023. "Efficient photodegradation of methyl red dye by kaolin clay supported zinc oxide nanoparticles with their antibacterial and antioxidant activities," *Heliyon,* 9(6): e16738, DOI: 10.1016/j.heliyon.2023.e16738.

[20] K. Song, X. Yu, D. Hu, X. Zheng, and J. Guo, 2013. "Photocatalytic degradation of ammonia nitrogen in aquaculture wastewater by using nano-ZnO," *Advanced Materials Research,* 610–613: 564–567. DOI: 10.4028/www.scientific.net/AMR.610-613.564.

[21] S. He et al., 2018. "High efficient visible-light photocatalytic performance of Cu/ZnO/rGO nanocomposite for decomposing of aqueous ammonia and treatment of domestic wastewater," *Frontiers in Chemistry*, 6: 219, DOI: 10.3389/fchem.2018.00219.

[22] D. Abu Bakar Sidik, N. H. H. Hairom, A. I. Rozman, M. J. S. Johari, and A. Muhammad, 2023. "The Photocatalytic Activity of Green Zinc Oxide Nanoparticles in the Treatment of Aerobically Palm Oil Mill Effluent," *Journal of Science and Technology,* 15(1): 7–15, DOI: 10.30880/jst.2023.15.01.002.

[23] D. Kanakaraju, M. S. Yahya, and S. P. Wong, 2019. "Removal of chemical oxygen demand from agro effluent by ZnO photocatalysis and photo-Fenton," *SN Applied Sciences*, 1(7): 1–9. DOI: 10.1007/s42452-019-0782-z.

[24] M. Irani, T. Mohammadi, and S. Mohebbi, 2016**.** "Photocatalytic degradation of methylene blue with ZnO nanoparticles: A joint experimental and theoretical study," *Journal of the Mexican Chemical Society*, 60(4): 218–225,